DOI: 10.2507/35th.daaam.proceedings.xxx

MODELLING INFLUENCE OF HEAT INPUT ON GMAW FILLET WELD GEOMETRY

Petar Tasić, Ismar Hajro, Adi Pandžić & Almira Softić

This Publication has to be referred as: Tasić, P[etar]; Hajro, I[smar]; Pandžić, A[di] & Softić, A[lmira] (2024). Modelling Influence of Heat Input on GMAW Fillet Weld Geometry, Proceedings of the 35th DAAAM International Symposium, pp.xxxx-xxxx, B. Katalinic (Ed.), Published by DAAAM International, ISBN 978-3-902734-xx-x, ISSN 1726-9679, Vienna, Austria
DOI: 10.2507/35th.daaam.proceedings.xxx

Abstract

One of the most often used welding processes in manufacturing components made of unalloyed structural steels is Gas Metal Arc Welding (GMAW). It is a relatively simple and cost-effective process providing high deposition rates and productivity. Moreover, it can be combined with other processes and/or fully robotized, both of which improve productivity even further. However, maintaining quality control of welds at these high productivity rates can be rather challenging task. There are standards describing the acceptance levels and corresponding weld quality, with some of the considered criteria based on the visible weld geometry. It would be beneficial to connect welding parameters with the weld geometry, so that deviation from defined geometry causes correction of welding parameters. This paper describes influence of heat input on leg size and penetration for GMAW fillet welds of unalloyed steel with thicknesses of 4 and 8 millimetres in horizontal position, with varied parameters being welding current and speed. Dependence is described through models based on linear regression analysis.

Keywords: GMAW, unalloyed steel, weld geometry, weld quality, model.

1. Introduction

Gas Metal Arc Welding (GMAW) is one of the most extensively used joining processes in (pre)fabrication of various structures. It can provide considerably higher productivity than Gas Tungsten Arc Welding (GTAW) or Shielded Metal Arc Welding (SMAW), due to its high deposition rates. [1] Furthermore, GMAW process can be easily modified or adapted for automation or robotisation. [2] This means improvement of working conditions and safety for welders. [3] Despite this, GMAW is still in significant portion used as manual welding process, increasing the possibility of introduction of flaws and defects caused the effect of human factors. [4] On the other side, such high deposition rates and, consequently, fast production of welds pose challenge regarding weld quality check. The easiest way to do it would be reliable control of heat input, i.e. essential welding parameters (welding current, voltage and welding speed). [5] Regardless, to achieve full control of welding process and its outcome, non-essential parameters (e.g. gas flow, inclination, contact tip to work distance) should be controlled as well. In this way, the same weld bead geometry features can be achieved all along the seam. [6] Controlling process parameters becomes particularly of interest when it comes to

Wire Arc Additive Manufacturing (WAAM), which is executed by deposition of metal layers on top of each other (like cladding). In these cases, control of the bead geometry is in significant portion control of product geometry. [7]

The idea of weld quality control through weld geometry control is not unknown, but it was used mostly for hybrid, beam and friction welding processes. As there are many recommendations for parameters selection for GMAW (and for arc processes in general), such relationships between the process parameters, the weld geometry and the weld quality are predominantly recently developed. [8] In many cases, driving forces are increased production volume and quality requirements on one side, and, on the other, reduction of manufacturing costs. Such concept of weld quality control relies on model, which has pivotal role in connecting welding process, heat input and weld geometry, as shown in Fig. 1.

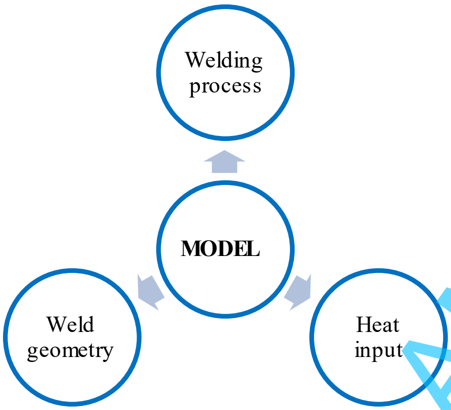

Fig. 1. Schematic representation of model connecting welding process, heat input and weld geometry [8]

Models describing weld geometry as function of heat input are relatively common. Some of the oldest models are based on corelation between leg size *z* (or weld thickness *a*) and heat input *Q* and are developed for welds of unalloyed structural steel made by arc processes, including GMAW. [9], [10] More recently, models are developed by using statistical tools (e.g. regression) for single process, one welding position and one type of steel, increasing model accuracy. [2], [11], [12] There are also doctoral theses dealing with prediction of geometry as function of heat input. [13], [14] Most recently, models are developed for GMAW using advanced statistical and mathematical tools, with strong potential for their implementation in manufacturing. The choice of process is driven by its widespread application in metalworking industry. [15], [16], [17] In some cases, models are coupled with real-time acquisition of weld geometry features by employing artificial vision, effectively establishing connection as shown in Fig. 1. [18], [19]

On the other side, models of heat input as function of weld geometry are scarce, but could be useful as well. For example, they could serve to enable on-line adjustment of parameters during welding to achieve certain weld geometry features, e.g. specified leg size *z* or weld thickness *a*, making such approach particularly useful in case of transitions between several welding position comprising single seam.

This study presents some of own experimental research conducted using GMAW process for single-pass fillet weld of non-alloyed structural steels with two thicknesses. Based on the results, the relationship between heat input and weld geometry has been established and evaluated by using statistical tools, with the purpose to see whether such relationship could be used in real manufacturing process.

2. Experimental research

To establish corelation between weld geometry features and heat input, a series of single-pass fillet welds on 4 mm and 8 mm thick plates of structural steels P355NL2 and S235JR (respectively) have been made using GMAW. Both steels are unalloyed low-carbon structural steels, with chemical composition given in Table 1 and mechanical properties given in Table 2.

	C	Mn	P	S	Si	Cu	N	Nb	Ni	Ti
S235JR	0.13	0.55	0.010	0.009	0.21	0.29	0.007	-	0.08	0.002
P355NL2	0.17	1.42	0.017	0.002	0.22	0.02	0.002	0.01	0.02	0.010

Table 1. Chemical composition (% wt.) of used steels [20], [21]

	Yield strength	Tensile strength	Elongation A_5	Impact toughness
S235JR	306 MPa	429 MPa	39%	149 J at -20 °C
P355NL2	435 MPa	555 MPa	32%	171 J at -20 °C

Table 2. Mechanical properties of used steels [20], [21]

Both steels have been chosen because of their widespread use for beams, supports, platforms, mine equipment, as well as in shipbuilding, and are known for excellent weldability and relatively low price. These thicknesses have been chosen as they are common for mentioned applications and can be used for single-pass fillet welds. All of them are made by using welding wire G 42 4 M21 3Si1 (EN ISO 14341-A) with diameter of 1.2 mm. Shielding gas in all experiments was pure CO_2, with flow varying from 13 to 17 litres/min, as recommended for GMAW. Contact Tip to Workplace Distance (CTWD) was kept between 12 and 15 mm, depending on current. All welds are made in flat position (PB), since it can support the biggest range of welding parameters.

There are three essential welding parameters for GMAW, namely welding current (*I*, A), arc voltage (*U*, V) and welding speed (*w*, cm/min). However, power source used in experiment was digitally controlled Daihen Welbee WB-P500L, with its electronics synergically corelating voltage with welding current, hence there were only two independent welding parameters, i.e. welding current and welding speed. Welding parameters were chosen to represent relatively wide range, with values measured during experiment given in Table 3.

	Welding current	**Arc voltage**	**Welding speed**	**Heat input**
4 mm	90 – 180 A	18.6 – 23.2 V	11 – 31 cm/min	0.33 – 1.05 kJ/mm
8 mm	165 – 190 A	22.2 – 28.5 V	14 – 61 cm/min	0.59 – 1.27 kJ/mm

Table 3. Welding parameters used in experiment

Heat input (*Q*, kJ/mm) is defined by (1), and for this experiment is calculated using average values of current and voltage measured by independently connected multimetar. Heat input efficiency η (also known as thermal efficiency) is usually taken based on recommendations, and in this case, it is η=0.8. [22], [23]

$$Q = \frac{I \cdot U}{w} \cdot \eta \tag{1}$$

All samples have been visually examined right after welding, with ones with significant visible imperfections being discarded and not considered in further analysis. Remaining samples have been cut, ground, polished and etched with nital. In that way, macro-sections of joints were prepared in accordance with EN ISO 17639. Afterwards, macro-sections were photographed, and geometry features analysed in AutoCAD, as shown in Fig. 2.

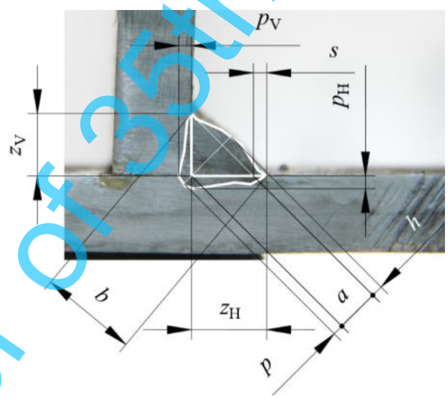

Fig. 2. Measurements and geometrical features visible at macro-section

Geometry features were measured in accordance with ISO/TR 25901-1, while weld imperfection tolerances for required quality levels were determined by ISO 5817. Additionally, two new geometry features are proposed. The one is average weld leg size z_a, described by (2) as average between leg size in horizontal (z_H) and vertical (z_V) direction. Similarly, average penetration p_a, described by (3), is average penetration between those in horizontal (p_H) and vertical (p_V) direction. The reason for introduction of average values is weld asymmetry. Ideally, there should be no asymmetry at all, but due to reality of manual welding process, it is always present, and it is considered as one of the representatives of weld quality. However, it is consequence of welder's manipulative abilities, and not heat input, and therefore omitted in this analysis.

$$z_a = \frac{z_H + z_V}{2} \tag{2}$$

$$p_a = \frac{p_H + p_V}{2} \tag{3}$$

3. Results and discussion

Based on the results of experiment, four models were developed for heat input, one as function of average leg size and other of average penetration, both for two thicknesses. Multiple linear regression has been used for this, as it was used in many previous research comparable to this one, and because problem is not too complex, including just few variables. Coefficients of regression models are obtained by the least squares method and are given in Table 4 and 5 for welds on 4 mm steel sheets, and Table 6 and 7 for 8 mm. Graphical representation of developed models are given.

	Coefficient	**Standard error**	***P*-value**
Intercept	-0.41881	0.08814	$5.47 \cdot 10^{-05}$
z_a (mm)	0.17778	0.01437	$7.27 \cdot 10^{-13}$

Table 4. Coefficients of regression model $Q=f(z_a)$ for 4 mm sheets

	Coefficient	**Standard error**	***P*-value**
Intercept	0.39433	0.07103	$6.15 \cdot 10^{-06}$
p_a (mm)	0.47230	0.11798	0.00042

Table 5. Coefficients of regression model $Q=f(p_a)$ for 4 mm sheets

	Coefficient	**Standard error**	***P*-value**
Intercept	-0.04303	0.12076	0.72429
z_a (mm)	0.13444	0.01715	$1.53 \cdot 10^{-08}$

Table 6. Coefficients of regression model $Q=f(z_a)$ for 8 mm sheets

	Coefficient	**Standard error**	***P*-value**
Intercept	0.74737	0.09075	$5.80 \cdot 10^{-09}$
p_a (mm)	0.11151	0.06562	0.10036

Table 7. Coefficients of regression model $Q=f(p_a)$ for 8 mm sheets

As possible to see, the *P*-values for intercept in Table 6 and p_a in Table 7 are bigger than 0.0500, meaning that intercept and p_a should have no effect on model's relevance, i.e. they are not statistically significant. Nevertheless, they are included in corresponding models due to physical nature of welding process being analysed. Basic data regarding regression analysis and developed models is given in Table 8.

	4 mm		**8 mm**	
	$Q=Q(z_a)$	$Q=Q(p_a)$	$Q=Q(z_a)$	$Q=Q(p_a)$
Coefficient of determination, R^2	0.84528	0.36401	0.68710	0.09348
Significance, *F*	$7.27 \cdot 10^{-13}$	0.00042	$1.53 \cdot 10^{-08}$	0.10036
Standard error	0.06669	0.13521	0.12712	0.21638
Number of experiments	30	30	30	30

Table 8. Results of regression models for two thicknesses

As possible to see from Table 8, significance *F* for model $Q=Q(p_a)$ for 8 mm has value of 0.10 (it is bigger than 0.05), what means that developed model is not sufficient to explain dependence of Q on p_a. Therefore, it will not be considered in further analysis. It is also possible to see that models based on average leg size have significantly bigger coefficient of determination (R^2) than those based on average penetration, meaning they are more reliable. Models for heat input as function of z_a and p_a are given with (4) and (5) for thickness of 4 mm, while (6) gives model of heat input as function of z_a for thickness of 8 mm.

$$Q = -0.41881 + 0.17778 \cdot z_a \quad (4)$$

$$Q = 0.39433 + 0.47230 \cdot p_a \quad (5)$$

$$Q = -0.04303 + 0.13444 \cdot z_a \quad (6)$$

Graphical interpretation of models given by (4), (5) and (6) is given in Fig. 3, 4 and 5, respectively. For comparison purposes, figures contain original experimental measurements as well.

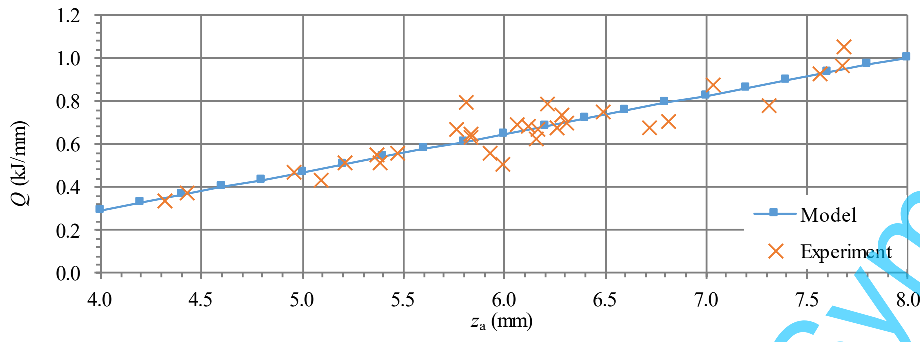

Fig. 3. Dependence of heat input on average leg size for thickness of 4 mm

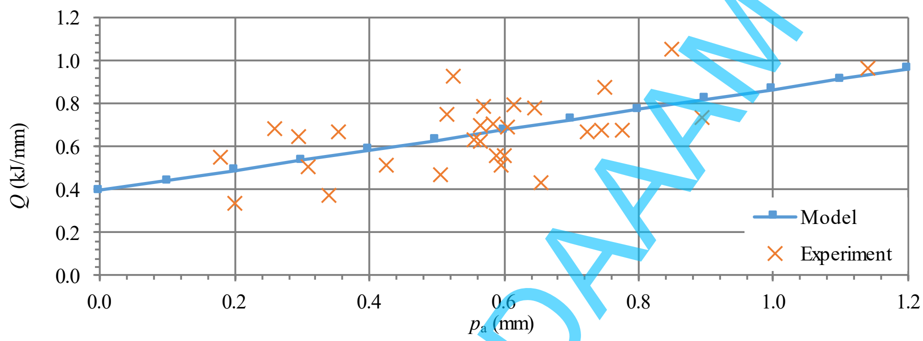

Fig. 4. Dependence of heat input on average penetration for thickness of 4 mm

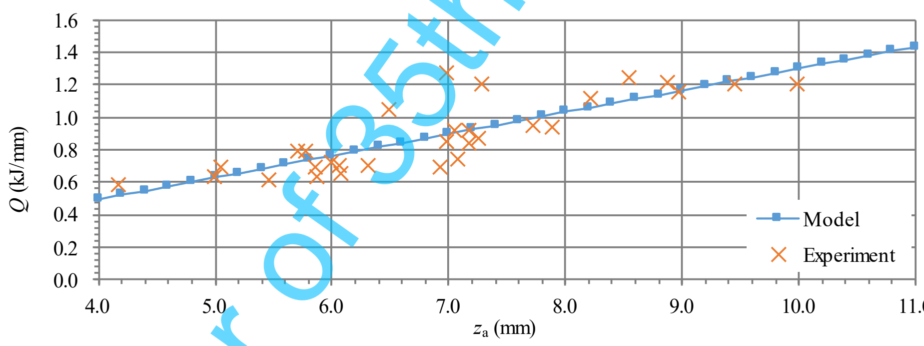

Fig. 5. Dependence of heat input on average leg size for thickness of 8 mm

Direct comparison between models for $Q=Q(z_a)$ for thicknesses 4 mm and 8 mm is given in Fig. 6.

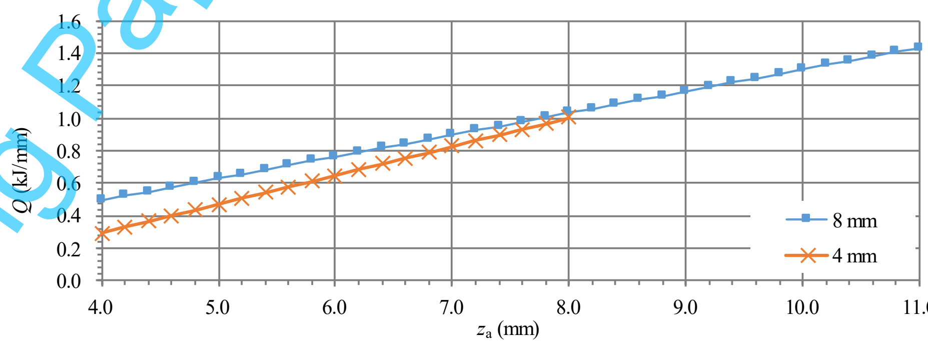

Fig. 6. Comparison of heat input models as function of average leg size for both thicknesses

It is noticeable that required heat input for 4 mm is lower than the one for 8 mm for the same average leg size, and that difference is more obvious as average leg size is smaller. Considering that the wire diameter is the same in both cases, and the difference between gas flows is insignificant, it is possible to conclude that the reason for difference lays in heat transfer in steel sheets. Due to difference in masses, thin sheet (4 mm) gets heated more rapidly than thick one (8 mm), hence more heat remains to melt filler metal, which, in turn, enables formation of weld with lower heat input.

According to models, for average leg size of approximately 8 mm, both models give the same heat input of about 1 kJ/mm. It should be noted that both current and welding speed affects heat input, and that the same value can be achieved with different combinations of them. However, from the technological point of view, having heat input of 1 kJ/mm on 4 mm thick steel sheet is rather extreme case, regardless the combination of current and welding speed, as it is on the verge of burning through the base metal.

4. Conclusion

Gas Metal Arc Welding is widely used process in making steel components and structures, primarily due to high productivity enabled by high deposition rates. Additionally, it is easily fully automated and/or coupled with robots, and it is also process that has many modifications. All this pushes productivity even further, requiring new ways to control welds. On the other side, it is process with no slag and with relatively small amount of fumes and dust, so it is suitable for coupling with artificial vision to scan welds and measure its geometry features in-situ in real time. That would maintain required weld quality level and increased productivity, leading to reduced costs. However, to implement this, the model connecting welding parameters (current, voltage and welding speed, heat input) with weld geometry and dimensions must be developed. In case such model is implemented in manufacturing process, parameters could be adjusted instantaneously during welding, enabling required weld profile along seams, even in cases of complex geometry and various welding positions.

This paper presents results of research on heat input dependence on two geometry features of welds. Experimental part of the study has been conducted making several series of fillet welds on unalloyed steel sheets with thicknesses of 4 mm and 8 mm, manually by using digitally controlled welding device and common filler metal and shielding gas. All welds were made in flat position, and afterward cut, polished and etched, so geometry features can be measured on prepared macrographs. For analysis, two of them were calculated, namely average leg size and average penetration. Each of these averaged values is calculated between values in horizontal and vertical direction. It is a new approach to define geometry features, as standards do not describe them, but rather consider welds with ideal geometry, i.e. symmetrical.

Based on experimental data, four models have been developed to describe heat input dependence on average leg size and penetration, for two thicknesses, with three of them proved to be statistically relevant. Models based on average leg size shown significantly higher coefficient of determination (R^2) than those based on average penetration. For both thicknesses, models shown that heat input does not strongly depend on average penetration, i.e. heat input has small or no influence on penetration. This is something that is opposite from real-life experience and physics of welding process, meaning it needs deeper and more detailed analysis. Models also shown that required average leg size can be achieved with smaller heat input on 4 mm than on 8 mm thick steel sheets, what is consequence of differences in heat transfer.

It would be possible to conclude that proposed approach of determining heat input as function of average leg size and average penetration has certain advantages, in particular if applied in manufacturing of steel structures, but still needs more data for verification and validation, and usage of improved or different statistical tools.

5. Further research

Further research have several possibilities, each of them with interesting perspective. On one side, it should focus on application of more advanced statistical tools that could provide better understanding of corelation between heat input and geometry features. On the other side, entire research can be reproduced, but this time using robot instead of welder. In this way, the welder's influence could be precisely determined. Further research could also include multi-pass welds, as well as welding stainless steels and aluminium alloys.

6. References

[1] Girón-Cruz, J. A., Pinto-Lopera, J. E. & Alfaro, S. C. A. (2022). Weld bead geometry real-time control in gas metal arc welding processes using intelligent systems, The International Journal of Advanced Manufacturing Technology, Vol. 123, 2022, pp. 3871-3884., DOI: 10.1007/s00170-022-10384-z

[2] Yaakub, M. Y., Tham, G., Rahim, W. M. A. W. A., Radzi, M. A. R. M. & Mahmud, A. (2013). Prediction of Welding Parameters and Weld Bead Geometry for GMAW Process in Overhead T-Fillet Welding Position(4F), Advanced Materials Research, Vol. 686, 2013, pp. 320-324., ISSN 1662-8985, DOI: 10.4028/www.scientific.net/AMR.686.320

[3] Popescu, M. (2010). Welding Ergonomics – Elements. Proceedings of the 21st International DAAAM Symposium, B. Katalinic (Ed.), Vol. 21, No. 1, ISSN 1726-9679

[4] Czifra, J., Vicikova, J. & Szabo, P. (2010). Automated production system for pipelines of vessels. Proceedings of the 21st International DAAAM Symposium, B. Katalinic (Ed.), Vol. 21, No. 1, ISSN 1726-9679

[5] Tham, G., Yaakub, M. Y., Abas, A. K., Manurung, Y. H. P. & Jalil, B. A. (2012). Predicting the GMAW 3F T-Fillet Geometry and Its Welding Parameter, Procedia Eng., Vol. 41, 2012, pp. 1794-1799., DOI: 10.1016/j.proeng.2012.07.385

[6] Filho, C. A. M. D., Sena, M. E. N., Neves, D. A., Brandi, S. D. & Neto, R. M. de A. C. (2023). Weld bead geometry prediction using artificial neural networks and genetic algorithm hybrid model in GMAW, Proceedings of 27th International Congress of Mechanical Engineering, 2023, DOI: 10.26678/ABCM.COBEM2023.COB2023-2140

[7] Maraki, M. R., Mahmoodi, M., Yousefieh M. & Tagimalek, H. (2023). Prediction and optimization of weld geometry in gas metal arc welding (GMAW) using least squares support vector machine, Journal of Welding Science and Technology of Iran, Vol. 8, 2023, ISSN: 2676-6787

[8] Tasic, P., Hajro, I., Hodzic, D. & Pandzic, A. (2020). Prediction of Geometry of Pulsed GMAW Fillet Welded Joints of Structural Steels. Proceedings of the 31st DAAAM International Symposium, pp.0444-0452, B. Katalinic (Ed.), ISBN 978-3-902734-29-7, ISSN 1726-9679, DOI: 10.2507/31st.daaam.proceedings.062

[9] Bosworth, M. R. (1991), Effective Heat Input in Pulsed Current Gas Metal Arc Welding with Solid Wire Electrodes, Welding Journal, Supplement, 1991, pp. 111-117

[10] Miller, D. K. & Funderburk R. S.(2001). Tools for reviewing Welding Procedures, Welding Journal, Vol. 80, No. 7, 2001, pp. 40-43., ISSN 0043-2296

[11] Gucwa, M. & Beczkowski, R. (2014). The Effect of Heat Input on the Geometric Properties of Welded Joints, Archivess of Foundry Engineering, Vol. 14, 2014, pp. 127-130., ISSN 1897-3310

[12] Ribeiro, R. A., Santos, E. B. F., Assunção, P. D. C., Maciel, R. R. & Braga E. M. (2015). Predicting Weld Bead Geometry in the Novel CWGMAW Process, Welding Journal, Vol. 94, No. 9, 2015, pp. 301-311., ISSN 0043-2296

[13] Khalaf, G. H. (1998). Neuro-fuzzy control modelling for gas metal arc welding process, Ph.D. Dissertation, Department of Manufacturing Engineering, Loughborough University, Loughborough, UK

[14] Benyounis, K. Y. (2006). Prediction and Optimization of Residual Stresses, Weld-Bead Profile and Mechanical Properties of Laser Welded Components, Ph.D. Dissertation, School of Mechanical and Manufacturing Engineering, Dublin City University, Dublin, Ireland

[15] Khrais, S., Al Hmoud, H., Al, A. A. & Darabseh, T. (2023). Impact of Gas Metal ArcWelding Parameters on Bead Geometry and Material Distortion of AISI 316L, Journal of Manufacturing and Materials Processing, Vol. 7, 2023, DOI: 10.3390/jmmp7040123

[16] He, Y., Li, D., Pan, Z., Ma, G. Yu, L., Yuan H. & Le, J. (2020). Dynamic Modeling ofWeld Bead Geometry Features in Thick Plate GMAW Based on Machine Vision and Learning, Sensors, Vol. 20, 2022, DOI: 10.3390/s20247104

[17] Biber, A., Sharma, R. & Reisgen, U. (2024). Robotic welding system for adaptive process control in gas metal arc Welding, Welding in the world, 2024, DOI: 10.1007/s40194-024-01756-y

[18] Lima, E. J., Castro, C., Bracarense, A. Q. & Campos M. M. (2005). Development of a model to predict weld bead geometry during the GMAW process using high speed camera. Proceedings of 7th International conference Trends in Welding Research, 2005

[19] Silva, R. H. G., Galeazzi, D., Schwedersky, M. B., Mendoça, F. K., Bonamigo, A. V. & Marques, C. (2021). An adaptive orbital system based on laser vision sensor for pipeline GMAW welding, Journal of the Brazilian Society of Mechanical Sciences and Engineering, Vol. 43, 2021, DOI: 10.1007/s40430-021-03081-7

[20] Inspection certificate 0083718076, dated 18.10.2023

[21] Inspection certificate 730/0045862, dated 29.04.2020

[22] Hajro, I. & Tasic, P. (2020). Influence of heat input and welding position on geometrical properties of GMAW fillet welds of unalloyed steel, TEM Journal, Vol. 9, No. 2, 2020, pp. 496-500., ISSN 2217-8309, DOI: 10.18421/TEM92-10

[23] Tasic, P.; Hajro, I. & Hodzic, D. (2017). Technological and Economical Aspects of Arc Welding of Al 5754, Proceedings of the 28th DAAAM International Symposium, pp.854-858, B. Katalinic (Ed.), Published by DAAAM International, ISBN 978-3-902734-11-2, ISSN 1726-9679, DOI: 10.2507/28th.daaam.proceedings.119